Chinese Chemical Letters 34 (2023) 108039

Contents lists available at ScienceDirect

Chinese Chemical Letters

journal homepage: www.elsevier.com/locate/cclet

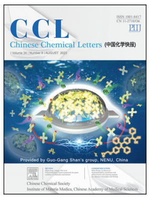

A new perchlorate-based hybrid ultramicroporous material with rich bare oxygen atoms for high C_2H_2/CO_2 separation

Ke Jiang[b,c], Yuntian Gao[a], Peng Zhang[a], Shiwei Lin[a], Ling Zhang[a,*]

[a] State Key Laboratory of Marine Resource Utilization in South China Sea, School of Materials Science and Engineering, Hainan University, Haikou 570228, China
[b] Key Laboratory of Food Nutrition and Functional Food of Hainan Province, School of Food Science and Engineering, Hainan University, Haikou 570228, China
[c] State Key Laboratory of Silicon Materials, Zhejiang University, Hangzhou 310027, China

ARTICLE INFO

Article history:
Received 16 August 2022
Revised 18 September 2022
Accepted 2 December 2022
Available online 5 December 2022

Keywords:
Porous materials
Gas separation
Pore chemistry
Flexibility
Host-guest interaction

ABSTRACT

Adsorptive separation of acetylene (C_2H_2) from carbon dioxide (CO_2) is of great significance in petrochemical industry, but still remains as a daunting challenge by reason of their very similar molecular sizes/shapes and physical properties. Herein, we reported a new perchlorate-based hybrid ultramicroporous material ZJU-194 that features the unique flexible-robust network decorated with rich bare oxygen atoms. By integrating the refined pore space as well as specific binding sites, the activated ZJU-194 (ZJU-194a) enables a selective two-step gate-opening adsorption toward C_2H_2, but blocks off the further uptake of CO_2. It thus exhibits a very high C_2H_2/CO_2 selectivity (22.4) at ambient conditions, which is superior to most reported MOF materials. Its complete separation for 50/50 C_2H_2/CO_2 mixtures is further evidenced by the dynamic breakthrough experiments.

Acetylene (C_2H_2), as an important industrial gas, has been widely used as feedstock for the production of commercial chemicals including acrylic acid, vinyl compounds and polyester plastic [1]. Typically, C_2H_2 comes from hydrocarbon cracking or methane combustion, thus inevitably coexisting with some of carbon dioxide (CO_2). Separation of C_2H_2 from C_2H_2/CO_2 mixtures is thus of great importance to obtain high-purity C_2H_2 for the subsequent manufacture processes. Due to their very similar molecular sizes/shapes (C_2H_2, 3.34 × 3.32 × 5.70 Å^3; CO_2, 3.33 × 3.18 × 5.36 Å^3, Fig. S1 in Supporting information) associated with close boiling points (C_2H_2, 189.3 K; CO_2, 194.7 K) [2], currently used cryogenic distillation and solvent extraction are energy-consuming and environment-unfriendly. Adsorptive separation by using porous materials thus offers a promising alternative approach for such C_2H_2 purification.

Microporous metal-organic frameworks (MOFs) also known as porous coordination polymers (PCPs) have attracted increased attention on various fields [3,4] including catalysis [5,6], sensing [7,8], biomedicine [9,10], especially for gas separation [11–13] owing to their readily tunable pore structure and functionality. Kitagawa's group reported the first MOF for C_2H_2/CO_2 separation in 2005 [14]. After this pioneering work, several MOFs that can selectively capture C_2H_2 [15–18] or CO_2 [19–22] from C_2H_2/CO_2 mixtures have been developed. The gas capture is generally driven by MOF network-gas interactions originating from the pore size and pore chemistry. Since C_2H_2 and CO_2 feature very similar molecular sizes/shapes, the pore confinement strategy of MOFs alone is quite limited to achieve high C_2H_2/CO_2 separation performance [23–26]. Hence, great efforts have been made to create functional sites including open metal sites [27], hydrogen-bonding acceptors [28–31], to selectively enforce the binding affinity towards C_2H_2. Those functionalized MOFs indeed provide large amount of C_2H_2 adsorption, while result in quite a few co-adsorption of CO_2 due to their enough large pore space. Optimizing pore size and functional surface simultaneously is thus pivotal for construction of the targeted MOFs for C_2H_2/CO_2 separation [32–34].

Recently, the well-known SIFSIX-type materials featuring anionic fluorinated groups (such as $SiF_6{}^{2-}$ and $NbOF_5{}^{2-}$) have been demonstrated as very promising materials for gas separation including CO_2/N_2 [35], C_2H_2/C_2H_4 [36], C_3H_4/C_3H_6 [37] and C_3H_6/C_3H_8 [38] separation, since their pore environments can be finely engineered. Whereas, such series of materials normally afford similar adsorption towards C_2H_2 and CO_2, as the fluoride atoms can form strong affinity to both of them, thus leading to moderate C_2H_2/CO_2 selectivity [39,40]. Compared with fluoride atoms, atoms with less negative charges might show increased

---

[*] Corresponding author.
E-mail address: ling.zhang@hainanu.edu.cn (L. Zhang).

https://doi.org/10.1016/j.cclet.2022.108039

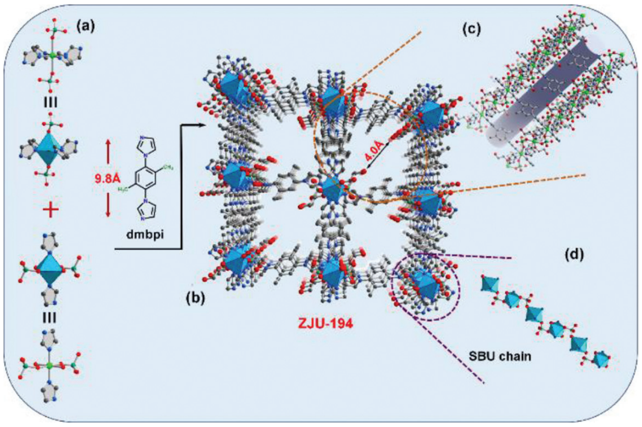

Fig. 1. The crystal structures of ZJU-194, (a) the coordination environments of Cu centers; (b) three-dimensional framework; (c) the rhomboid channel viewed along *a* axis; (d) the Cu node chains along *a* axis (C, gray; O, red; N, blue; Cl, green; Cu, cyan; H atoms are omitted for the clarity.

recognition for C_2H_2 *versus* CO_2. In particular, oxygen atoms have been well-established to form strong hydrogen-bonding with C_2H_2 molecules, but relatively weaker electrostatics with CO_2 molecules [41,42].

With this in mind, we have firstly introduced ClO_4^- as the inorganic linker, imidazole derivative dmpbi (dmpbi = 1,1′-(2,5-dimethyl-1,4-phenylene)bis(1*H*-imidazole)) as the organic linker, and successfully constructed a new perchlorate-based hybrid ultra-microporous material ZJU-194 $[Cu(dmpbi)_{1.5}(ClO_4)(C_2H_5O_2)]_n$ (CCDC No. 2,050,515). Notably, ZJU-194 possesses the flexible-robust network with one-dimensional tight channels lined with rich bare oxygen atoms. By integrating the refined pore space as well as specific binding sites, the activated ZJU-194 (ZJU-194a) enables a selective two-step gate-opening behavior toward C_2H_2 over CO_2. It thus affords very high adsorptive selectivity for C_2H_2/CO_2 (22.4) at ambient conditions, which is even comparable to the benchmark FeNi-M'MOF (24.0) [32] and MOF-OH (25.0) [43], and superior to most MOFs. Dynamic breakthrough experiments further suggest that the complete C_2H_2/CO_2 separation and high-purity C_2H_2 production can be achieved by ZJU-194a.

Reaction of dmpbi ligand with $Cu(ClO_4)_2 \cdot nH_2O$ yielded blue sheet-shaped crystals ZJU-194, and the phase purity was further confirmed by powder X-ray diffraction analysis (PXRD) (Fig. S2 in Supporting information). Crystal analyses clearly show that ZJU-194 crystallizes in triclinic P_{-1} space group (Fig. S3 and Table S1 in Supporting information). Both dmpbi ligands and ClO_4^- groups are two-connected with Cu atoms, while all Cu centers serve as six-connected nodes, but fall into two different coordination models (Fig. 1a). One type Cu atom connects with four independent dmpbi ligands and two ClO_4^- anions, and the other is coordinated by two dmpbi ligands, two ClO_4^- anions and two glycol molecules. Both Cu nodes arrange alternatively and are linked adjacently by one ClO_4^- anion, thus resulting in one-dimensional (1D) chains (Fig. 1d). Such chains are further bridged by dmpbi ligands to form the 3D network, generating the rhomboid channels with the cavity size of ~4.0 Å (Figs. 1b and c). Moreover, the pore walls are lined by rich bare oxygen atoms originated from ClO_4^- anions and the coordinated glycol molecules. These rich bare oxygen atoms within tight cavities can induce strong electrostatics field that would benefit for further gas storage and separation.

We first evaluated the stability of ZJU-194, since the industrial C_2H_2 streams typically contain some moisture. As shown in Fig. S5 (Supporting information), ZJU-194 can keep its structure stable even after soaking in water for 1 day, thus revealing its remarkable chemical stability. It also suggests the good thermostability of ZJU-194, as no decomposition of framework occurs up to 305 °C (Fig. S6 in Supporting information). After solve-exchange, ZJU-194 was evacuated at room temperature for 1 day to yield the activated sample (termed as ZJU-194a). PXRD analyses reveal that ZJU-194a still holds its crystalline nature, but shows different patterns from the original ones (Fig. S2). Such similar changes have been widely observed in some MOFs with flexible networks like MIL-53 [44], UTSA-300 [45] and ZJU-196 [46]. It means a probably flexible network of ZJU-194a. To proof such speculation, the molecular probe CO_2 and C_2H_2 were utilized for gas sorption experiments at 196 K (Fig. S7 in Supporting information). Specifically, ZJU-194a shows a typical two-step gate-opening adsorption for CO_2, of which the uptake at the first step (0–0.46 bar) is up to 34.7 cm^3/g, and the second step finally affords the adsorption capacity of 43.0 cm^3/g at 1.0 bar. The corresponding Brunauer–Emmett–Teller (BET) was estimated to be 108.7 m^2/g. Notably, such well-defined plateau of the adsorption isotherm clearly reveals the flexible-robust network of ZJU-194a. Conversely, fast adsorption of C_2H_2 in ZJU-194a was achieved at 196 K with the saturated capacity of ~60 cm^3/g at 0.03 bar. It thus indicates the much stronger C_2H_2-ZJU-194a interaction than that of CO_2.

Single-component equilibrium sorption isotherms of C_2H_2 and CO_2 were obtained at 273 K and 296 K respectively (Fig. 2a). Notably, both C_2H_2 adsorption isotherms exhibit two-step uptake behaviors. For 273 K, the C_2H_2 uptake at the first step (0–0.12 bar) is up to 0.91 mmol/g, probably driven by the intrinsic microporous cavies of the robust dense-phase structure [47]. The second step starts at around 0.12 bar and finally affords a C_2H_2 adsorption capacity of 2.42 mmol/g at 1.0 bar. As expected, the gate-opening pressure shifts to higher value (0.32 bar) when the temperature rises up to 296 K. The C_2H_2 adsorption amount of ZJU-194a (1.74 mmol/g at 296 K and 1.0 bar) is comparable to the benchmark CPL-1-NH_2 (1.84 mmol/g) [48] and JNU-1 (2.10 mmol/g) [49], and greatly outperforms that of iMOF-6C (1.11 mmol/g) [50]. Conversely, CO_2 is incapable to trigger the gate-opening adsorption at both 273 K and 296 K, with quite minor uptake capacity of ~0.5 mmol/g at 1.0 bar. For 50/50 C_2H_2/CO_2 separation, the C_2H_2/CO_2 uptake ratio at 0.5 bar is also important. Due to the exclusion effect towards CO_2, ZJU-194a shows very high C_2H_2/CO_2 uptake ratio (4.03) at 0.5 bar, which is superior to most of best-performing MOFs, such as UTSA-74 (2.03) [27], BUT-85 (3.56) [29], FeNi-M'MOF (2.01) [32], NKMOF-1-Ni (1.25) [33], TCuCl (1.96) [51], ZNU-1 (2.46) [52], SNNU-45 (2.03) [53] and MUF-17 (1.25) (Fig. 2b) [54]. Such well-controlled gate-opening adsorption of C_2H_2 *versus* CO_2 endows ZJU-194a as a desired C_2H_2-selective adsorbent.

Encouraged by the obvious uptake differences of ZJU-194a, we employed the well-established Ideal Adsorbed Solution Theory (IAST) to estimate its adsorption selectivity for 50/50 (v/v) C_2H_2/CO_2 mixtures (Fig. 3a and Figs. S9-S12 in Supporting information). For the very challenging C_2H_2/CO_2 separation, ZJU-194a shows an ultrahigh selectivity up to 125.0 at 0.01 bar (Fig. 3d). With the increase of pressure, the selectivity gradually decreases down to 22.4 at 1.0 bar. We further made comparison of C_2H_2/CO_2 selectivity at ambient conditions among reported MOFs with various separation mechanisms. Clearly, as shown in Fig. 3b, it is hardly for those MOFs to achieve high C_2H_2/CO_2 selectivity (> 20) based on a single separation mechanism including OMS, H-binding and pore confinement [55–60]. On the contrary, the combined effects of OMS or H-binding with pore confinements afford the increased C_2H_2/CO_2 selectivity [61–66]. Actually, most leading MOFs for C_2H_2/CO_2 separation are those with tight binding sites within small pores. Especially, those ultramicroporous MOFs with high density OMS exhibit the benchmark C_2H_2/CO_2 selectivity including ZJU-74a [32] and ATC-Cu [15]. Whereas, it seems more challenging for MOFs to achieve benchmark C_2H_2/CO_2 selectivity *via* H-binding combined with pore confinement effects, as most of them show

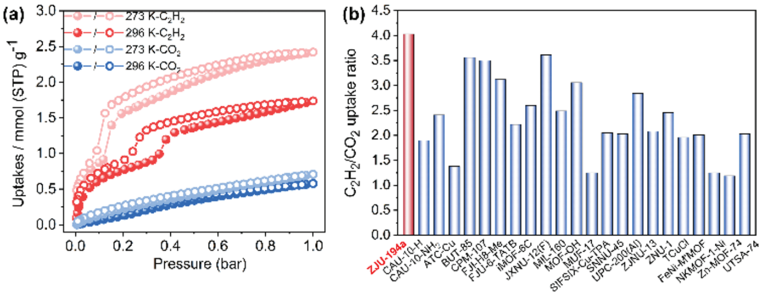

Fig. 2. (a) Single-component sorption isotherms of C_2H_2 and CO_2 for ZJU-194a. (b) Comparison of the C_2H_2/CO_2 uptake ratio of ZJU-194a with other promising materials at 0.5 bar and room temperature.

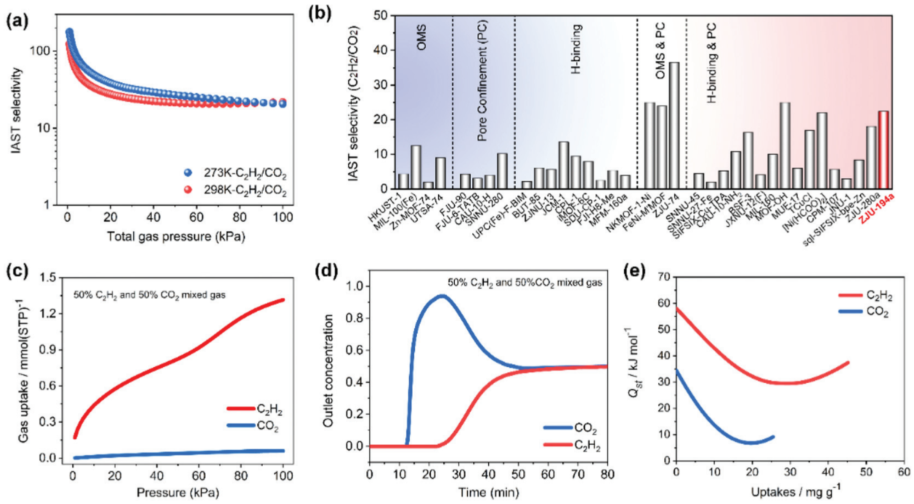

Fig. 3. (a) IAST calculations of ZJU-194a for the C_2H_2/CO_2 (50:50, v/v) separation at 296 K. (b) Comparison of the C_2H_2/CO_2 selectivity at room temperature and 1.0 bar among some promising MOFs. (c) IAST calculated C_2H_2 and CO_2 uptake isotherms of ZJU-194a from C_2H_2/CO_2 (50:50, v:v) gas mixtures at 296 K. (d) Dynamic breakthrough curves of ZJU-194a for the C_2H_2/CO_2 (50/50) separation at 296 K with a constant flow rate of 2 mL/min. (e) The isosteric heat (Q_{st}) of C_2H_2 and CO_2 adsorption for ZJU-194a.

moderate selectivity. In particular, although some MOFs with large pores exhibit extremely high C_2H_2 uptake capacity such as SNNU-45 [53], MOF-160 [63,64] and ZJNU-117 [67], their C_2H_2/CO_2 selectivity are still lower than that of ZJU-194a. Moreover, the C_2H_2/CO_2 selectivity of ZJU-194a is even comparable to the benchmark MOFs with high density OMS such as FeNi-M'MOF (24) [32] and NKMOF-1-Ni (~22) [33], and much higher than most reported promising materials including BUT-85 (6.1) [29], MUF-17 (6.0) [54], JCM-1 (13.7) [56], CAU-10-NH_2 (10.8) [58], TCuCl(16.9) [51], UTSA-74 (9.0) [27] and FJU-6-TATB (4.3) (Fig. 3e) [24]. We further obtained the static uptake isotherms of C_2H_2 and CO_2 from equimolar C_2H_2/CO_2 mixtures based on IAST calculations. As shown in Fig. 3c and Fig. S13 (Supporting information), ZJU-194a gives high adsorption capacity of C_2H_2 (1.97 mmol/g and 1.32 mmol/g for 273 K and 296 K respectively) at 1.0 bar while almost completely excluding CO_2, further indicating its particular promise for C_2H_2/CO_2 separation. Dynamic breakthrough test was thus conducted to evaluate the feasibility of ZJU-194a for equimolar C_2H_2/CO_2 mixtures. Clearly, the efficient separation can be accomplished by ZJU-194a. As shown in Fig. 3d, CO_2 eluted first from the column, while C_2H_2 could be detected after 23 min. The regeneration curves of ZJU-194a were obtained *via* purging by He flow (5 mL/min) at 308 K. As illustrated in Fig. S15 (Supporting information), 96% CO_2 could be desorbed within 5 min, while it needs 35 min to totally remove C_2H_2 from the breakthrough column. In addition, the C_2H_2 production is estimated to be 0.77 mmol/g for one cycle, and the recovered purity reaches up to 80%.

The C_2H_2-selective capture from C_2H_2/CO_2 mixtures by ZJU-194a could be explained by the different host-guest affinity, which is reflected in the isoteric heat of adsorption (Q_{st}). We thus evaluated the Q_{st} of C_2H_2 and CO_2 in ZJU-194a by calculating the gas adsorption isotherms at different temperature (Figs. S16 and S17 in Supporting information). As shown in Fig. 3e, the Q_{st} values of C_2H_2 at near zero loading is as high as 58.1 kJ/mol, notablely higher than that of CO_2 (34.4 kJ/mol). It thus reveals the much stronger interaction between the empty network of ZJU-194a and C_2H_2 than that of CO_2. Particularly, such high Q_{st} value of ZJU-194a for C_2H_2 is comparable to and even higher than those of MOFs with high density OMS, such as Fe-MOF-74 (47 kJ/mol) [68], NKMOF-1-Ni (60.3 kJ/mol) [33], and ZJU-74a (45 kJ/mol) [34].

In summary, we have designed a new perchlorate-based hybrid ultramicroporous material for high C_2H_2/CO_2 separation. By integrating the refined pore space as well as rich bare oxygen atoms, ZJU-194a enables a selective two-step gate-opening behavior toward C_2H_2, but blocks off the adsorption of CO_2. It thus affords a very high adsorptive selectivity for C_2H_2/CO_2 (22.4) at ambient conditions, which is superior to most MOFs. Both single-component equilibrium sorption and dynamic breakthrough experiments reveal its high C_2H_2 capture and C_2H_2/CO_2 separation performance. Our work here provides a new view of regulating the pore chemistry and the flexible-robust network comprehensively within MOF adsorbents to address the very challenging C_2H_2 separation.

Declaration of competing interest

The authors declare no competing financial interest.

Acknowledgments

This work was supported by the National Natural Science Foundation of China (No. 52003069) and the Hainan Provincial Natural Science Foundation of China (No. 520QN220).

Supplementary materials

Supplementary material associated with this article can be found, in the online version, at doi:10.1016/j.cclet.2022.108039.

References

[1] A. Granada, S.B. Karra, S.M. Senkan, Ind. Eng. Chem. Res. 26 (1987) 1901–1905.
[2] J.R. Li, R.J. Kuppler, H.C. Zhou, Chem. Soc. Rev. 38 (2009) 1477–1504.
[3] H. Furukawa, K.E. Cordova, M. O'Keeffe, O.M. Yaghi, Science 341 (2013) 1230444.
[4] H.C. Zhou, S. Kitagawa, Chem. Soc. Rev. 43 (2014) 5415–5418.
[5] H.F. Wang, L. Chen, H. Pang, S. Kaskel, Q. Xu, Chem. Soc. Rev. 49 (2020) 1414–1448.
[6] L. Zhang, J. Wang, K. Jiang, et al., Angew. Chem. Int. Ed. (2022) e202214794.
[7] Y. Cui, J. Zhang, H. He, G. Qian, Chem. Soc. Rev. 47 (2018) 5740–5785.
[8] D. Yue, J. Zhu, D. Chen, et al., Dyes Pigments 206 (2022) 110655.
[9] W. Ni, K. Jiang, Q. Ke, et al., J. Mater. Sci. Technol. 141 (2023) 11–20.
[10] J. Su, P. Jing, K. Jiang, J. Du, Dalton Trans. 51 (2022) 8938–8944.
[11] W.G. Cui, T.L. Hu, X.H. Bu, Adv. Mater. 32 (2020) e1806445.
[12] L. Yang, S. Qian, X. Wang, et al., Chem. Soc. Rev. 49 (2020) 5359–5406.
[13] S. Chen, S. Lin, L. Zhang, Mater. Lett. 327 (2022) 133064.
[14] R. Matsuda, R. Kitaura, S. Kitagawa, et al., Nature 436 (2005) 238–241.
[15] Z. Niu, X. Cui, T. Pham, et al., Angew. Chem. Int. Ed. 60 (2021) 5283–5288.
[16] L. Zhang, K. Jiang, L. Yang, et al., Angew. Chem. Int. Ed. 60 (2021) 15995–16002.
[17] J. Wang, Y. Zhang, Y. Su, et al., Nat. Commun. 13 (2022) 200.
[18] Y. Yang, H. Zhang, Z. Yuan, et al., Angew. Chem. Int. Ed. (2022) e202207579.
[19] Y. Xie, H. Cui, H. Wu, et al., Angew. Chem. Int. Ed. 60 (2021) 9604–9609.
[20] O.T. Qazvini, R. Babarao, S.G. Telfer, Nat. Commun. 12 (2021) 197.
[21] L.Z. Cai, Z.Z. Yao, S.J. Lin, M.S. Wang, G.C. Guo, Angew. Chem. Int. Ed. 60 (2021) 18223–18230.
[22] L. Li, J. Wang, Z. Zhang, et al., ACS Appl. Mater. Interfaces 11 (2019) 2543–2550.
[23] J. Pei, H.M. Wen, X.W. Gu, et al., Angew. Chem. Int. Ed. 60 (2021) 25068–25074.
[24] L. Liu, Z. Yao, Y. Ye, et al., J. Am. Chem. Soc. 142 (2020) 9258–9266.
[25] X. Mu, Y. Xue, M. Hu, et al., Chin. Chem. Lett. 34 (2023) 107296.
[26] T. Xu, M. He, L. Fan, et al., Dalton Trans. 50 (2021) 638–646.
[27] F. Luo, C. Yan, L. Dang, et al., J. Am. Chem. Soc. 138 (2016) 5678–5684.
[28] W. Fan, S. Yuan, W. Wang, et al., J. Am. Chem. Soc. 142 (2020) 8728–8737.
[29] G.R. Si, W. Wu, T. He, et al., ACS Mater. Lett. 4 (2022) 1032–1036.
[30] T. Li, P. Cui, D. Sun, Inorg. Chem. 61 (2022) 4251–4256.
[31] X. Wang, L. Yue, P. Zhou, L. Fan, Y. He, Inorg. Chem. 60 (2021) 17249–17257.
[32] J. Gao, X. Qian, R.B. Lin, et al., Angew. Chem. Int. Ed. 59 (2020) 4396–4400.
[33] Y.L. Peng, T. Pham, P. Li, et al., Angew. Chem. Int. Ed. 57 (2018) 10971–10975.
[34] J. Pei, K. Shao, J.X. Wang, et al., Adv. Mater. 32 (2020) e1908275.
[35] P. Nugent, Y. Belmabkhout, S.D. Burd, et al., Nature 495 (2013) 80–84.
[36] X. Cui, K. Chen, H. Xing, et al., Science 353 (2016) 141–144.
[37] L. Li, H.M. Wen, C. He, et al., Angew. Chem. Int. Ed. 57 (2018) 15183–15188.
[38] A. Cadiau, K. Adil, P.M. Bhatt, Y. Belmabkhout, M. Eddaoudi, Science 353 (2016) 137–140.
[39] H. Li, C. Liu, C. Chen, et al., Angew. Chem. Int. Ed. 60 (2021) 7547–7552.
[40] K.J. Chen, H.S. Scott, D.G. Madden, et al., Chem 1 (2016) 753–765.
[41] H.S. Scott, M. Shivanna, A. Bajpai, et al., ACS Appl. Mater. Interfaces 9 (2017) 33395–33400.
[42] L. Zhang, K. Jiang, J. Zhang, et al., ACS Sustain. Chem. Eng. 7 (2018) 1667–1672.
[43] W. Gong, H. Cui, Y. Xie, et al., J. Am. Chem. Soc. 143 (2021) 14869–14876.
[44] T. Loiseau, C. Serre, C. Huguenard, et al., Chem. Eur. J. 10 (2004) 1373–1382.
[45] R.B. Lin, L. Li, H. Wu, et al., J. Am. Chem. Soc. 139 (2017) 8022–8028.
[46] L. Zhang, K. Jiang, L. Li, et al., Chem. Commun. 54 (2018) 4846–4849.
[47] Y. Gu, J.J. Zheng, K.I. Otake, et al., Angew. Chem. Int. Ed. 59 (2020) 15517–15521.
[48] L. Yang, L. Yan, Y. Wang, et al., Angew. Chem. Int. Ed. 60 (2021) 4570–4574.
[49] H. Zeng, M. Xie, Y.L. Huang, et al., Angew. Chem. Int. Ed. 58 (2019) 8515–8519.
[50] S. Dutta, S. Mukherjee, O.T. Qazvini, et al., Angew. Chem. Int. Ed. 61 (2022) e202114132.
[51] S. Mukherjee, Y. He, D. Franz, et al., Chem. Eur. J. 26 (2020) 4923–4929.
[52] L. Wang, W. Sun, Y. Zhang, et al., Angew. Chem. Int. Ed. 60 (2021) 22865–22870.
[53] Y.P. Li, Y. Wang, Y.Y. Xue, et al., Angew. Chem. Int. Ed. 58 (2019) 13590–13595.
[54] O.T. Qazvini, R. Babarao, S.G. Telfer, Chem. Mater. 31 (2019) 4919–4926.
[55] M. Fischer, F. Hoffmann, M. Froba, ChemPhysChem 11 (2010) 2220–2229.
[56] J. Lee, C.Y. Chuah, J. Kim, et al., Angew. Chem. Int. Ed. 57 (2018) 7869–7873.
[57] W.J.F. Trenholme, D.I. Kolokolov, M. Bound, et al., J. Am. Chem. Soc. 143 (2021) 3348–3358.
[58] T. Xu, Z. Jiang, P. Liu, et al., ACS Appl. Nano Mater. 3 (2020) 2911–2919.
[59] Z. Di, C. Liu, J. Pang, et al., Angew. Chem. Int. Ed. 60 (2021) 10828–10832.
[60] Y. Ye, Z. Ma, R.B. Lin, et al., J. Am. Chem. Soc. 141 (2019) 4130–4136.
[61] Y. Zhang, J. Hu, R. Krishna, et al., Angew. Chem. Int. Ed. 59 (2020) 17664–17669.
[62] X. Zhang, R.B. Lin, H. Wu, et al., Chem. Eng. J. 431 (2022) 134184.
[63] Y.M. Gu, H.F. Qi, T.T. Sun, et al., Chem. Mater. 34 (2022) 2708–2716.
[64] Y. Ye, S. Xian, H. Cui, et al., J. Am. Chem. Soc. 144 (2022) 1681–1689.
[65] Q.L. Qian, X.W. Gu, J. Pei, et al., J. Mater. Chem. A 9 (2021) 9248–9255.
[66] X.P. Fu, Y.L. Wang, X.F. Zhang, et al., Chem. Eng. J. 432 (2022) 134433.
[67] L. Fan, L. Yue, W. Sun, et al., ACS Appl. Mater. Interfaces 13 (2021) 40788–40797.
[68] E.D. Bloch, W.L. Queen, R. Krishna, et al., Science 335 (2012) 1606–1610.